

A Peierls Criterion for the Onset of Deformation Twinning at a Crack Tip

E.B. Tadmor^{*}, S. Hai

*Department of Mechanical Engineering, Technion – Israel Institute of Technology,
32000 Haifa, Israel.*

Abstract

A criterion for the onset of deformation twinning (DT) is derived within the Peierls framework for dislocation emission from a crack tip due to Rice (1992). The critical stress intensity factor (SIF) is obtained for nucleation of a two-layer microtwin, which is taken to be a precursor to DT. The nucleation of the microtwin is controlled by the *unstable twinning energy* γ_{ut} , a new material parameter identified in the analysis. γ_{ut} plays the same role for DT as γ_{us} , the unstable stacking energy introduced by Rice, plays for dislocation emission. The competition between dislocation emission and DT at the crack tip is quantified by the *twinning tendency* T defined as the ratio of the critical SIF's for dislocation nucleation and microtwin formation. DT is predicted when $T > 1$ and dislocation emission when $T < 1$. For the case where the external loading is proportional to a single load parameter, T is proportional to $\sqrt{\gamma_{\text{us}}/\gamma_{\text{ut}}}$. The predictions of the criterion are compared with atomistic simulations for aluminum of Hai and Tadmor (2003) for a number of different crack configurations and loading modes. The criterion is found to be qualitatively exact for all cases, predicting the correct deformation mode and activated slip system. Quantitatively, the accuracy of the predicted nucleation loads varies from 5% to 56%. The sources of error are known and may be reduced by appropriate extensions to the model.

Key words: A.crack tip plasticity, A.dislocations, A.twinning, C.conservative integrals, Peierls concept

1 Introduction

Models for the initiation of deformation twinning (DT) may be broadly divided into two categories: homogeneous and heterogeneous nucleation (Chris-

^{*} Corresponding author; email: tadmor@tx.technion.ac.il; fax: +(972) 4-832-4533

Christian and Mahajan, 1995). Homogeneous nucleation models assume that a twin nucleus is formed in a region of near perfect crystal under the action of an external stress. Criteria for homogeneous nucleation of deformation twins have been derived in various ways including (1) uniform shear of the lattice to its twin counterpart (Paxton et al., 1991); (2) treatment of the twin as a mode II slit and application of a Griffith-type criterion for its extension (Yoo, 1979); (3) treatment of the twin as an ellipsoid embedded in a strained anisotropic medium and application of an energy minimization criterion (Lebensohn and Tomé, 1993a); and (4) dislocation modelling of a twin lamella at a free surface (Jagannadham et al., 1993). A general conclusion to emerge from these models is that the energy barrier for homogeneous nucleation is too large to be supplied by thermal fluctuations alone (Christian and Mahajan, 1995; Lebensohn and Tomé, 1993a). For the barrier to drop to an acceptable level, very large stresses, either externally applied or due to internal stress concentrations, are required. Given this, it is perhaps more reasonable to assume heterogeneous nucleation of twins at pre-existing defect sites. Potential sites for twin nucleation include grain boundaries, dislocations and dislocation pile-ups, surfaces and crack tips (Yoo, 1998). Most of the work on heterogeneous nucleation has focused on dislocation-based nucleation criteria which postulate various dislocation reactions that could lead to the formation of a twin (see Christian and Mahajan (1995) for a review of different proposed mechanisms). Far less attention has been given to nucleation at grain boundaries, surfaces and crack tips. This paper focuses on cracks.

It is well-known that crack tips can serve as nucleation sites for deformation twins. Experimental investigations of cleavage in metals that exhibit DT often find twins in the vicinity of the crack faces (Deruyttere and Greenough, 1954; Reid, 1981). The formation of deformation twins at crack tips has also been observed directly, in situ, in TEM (Pond and Garcia-Garcia, 1981; Chen et al., 1999). DT at crack tips can have a strong influence on the fracture of a material. In titanium aluminides, DT has the positive effect of increasing the fracture toughness of the material (Dève and Evans, 1991). In ferritic steels the effect is opposite. In these materials crack propagation occurs by the nucleation of twins ahead of the crack tip which subsequently serve as nucleation sites for further cleavage (Bošanský and Šmida, 2002). DT can also result in the blunting of crack tips (Yoo, 1998). An analytical criterion for DT at a crack tip could offer valuable information on these processes and help to elucidate the role of DT in crack propagation (Yoo, 1981).

To our knowledge, the only published theoretical analysis of DT at a crack tip appears in the pioneering study of Bilby and Bullough (1954). The authors obtain an analytical solution for the stress state at the tip of a moving crack under general applied loading. They then assume that twinning is controlled by the resolved shear stress on the twin plane in the twinning direction. No specific criterion for twin nucleation is adopted. Rather the authors identify the

twin planes and directions where the resolved mode II stress intensity factor (SIF) is in the correct direction for twinning and of the largest magnitude, and suggest that twinning is more likely to occur on these systems. The theory is applied to the fracture of hcp zinc single crystals and its predictions are found to be in excellent agreement with the experiments of Deruyttere and Greenough (1954) on the same material.

In this paper we present a quantitative criterion for the onset of DT at the tip of a static crack in a single crystal. The work was motivated by the atomistic simulations of cracks in fcc aluminum of Hai and Tadmor (2003), which show that the deformation mechanism at the crack tip (dislocation emission vs. DT) strongly depends on the system crystallography and loading mode. The atomistic simulations were carried out on straight plane strain cracks. The twins that were nucleated in the simulations always formed by layer-by-layer emission of Shockley partial dislocations from the crack tip. This is the mechanism of twin formation considered here. The criterion is derived within the Peierls framework for dislocation emission from a crack tip introduced by Rice (1992) and serves as an extension of that work.

In section 2 we describe the underlying principles of the model showing how the Rice model for dislocation emission may be extended to twinning and we derive the DT criterion. In order to minimize confusion we conform as much as possible to the notation introduced by Rice (1992). In section 3 we compare the predictions of the criterion to the atomistic study of Hai and Tadmor (2003) mentioned above. We also construct yield envelopes for DT vs. dislocation emission for cases of mixed mode loading.

2 Peierls Framework for Deformation Twinning at a Crack Tip

2.1 Description of Model

We consider a remotely-loaded, atomically-sharp crack in a single crystal material. Fig. 1 shows a closeup of the crack tip region. K-dominance (Suresh, 1991) is assumed to hold so that the stresses in the vicinity of the crack tip are characterized by the SIF's K_I , K_{II} and K_{III} as indicated schematically in the figure. We limit ourselves to configurations where a slip plane intersects the crack front and are interested in obtaining the critical SIF's necessary to nucleate defects on this plane. In particular, we focus on the competition between the nucleation of a dislocation on the intersecting slip plane and the formation of a twin on the same set of planes. The assumption of K-dominance for the configurations studied here is quite reasonable and has repeatedly been born out by atomistic calculations that show that linear elastic behavior is recov-

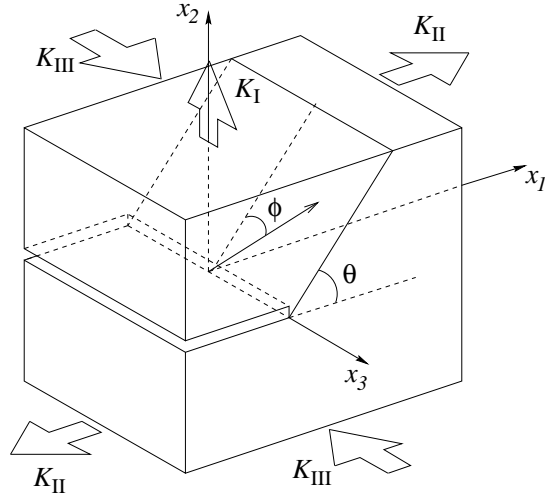


Fig. 1. A schematic diagram of the crack tip region showing the inclined slip plane and slip direction posited by the dislocation nucleation model.

ered several lattice spacings away from the crack tip (see for example Miller et al. (1998)). The only limitation implied by K-dominance is that the size of the slipped region expected at the crack tip must be small relative to the length of the crack, and to distances from the crack tip to the model boundaries and points of application of the external load. The more constricting assumption is that a slip plane intersects the crack front. This is mitigated to some extent by the fact that a crack front can always deviate locally to come into coincidence with a slip plane for the purpose of nucleating a dislocation (Rice et al., 1992). Fig. 1 also gives the geometric parameters of the model: θ is the angle of inclination of the slip plane relative to the crack plane and ϕ is the angle of the slip direction relative to the normal to the crack front. For a dissociated dislocation comprised of two partial dislocations, we define ϕ_A as the slip direction of the leading partial and ϕ_B as the slip direction of the trailing partial.

The problem of dislocation nucleation from the crack tip configuration of Fig. 1 was solved by Rice (1992). Rice's analysis is based on the Peierls (1940) concept, whereby a periodic relation is assumed to hold between the shear stress and slip discontinuity along the dominant slip direction ahead of the crack tip. By making use of the J-Integral (Rice, 1968), Rice obtained a closed-form solution for the critical SIF's required to emit a dislocation. The solution is exact (within the Peierls concept approximation) for the case where the slip plane ahead of the crack tip is coplanar with the crack and the loading direction coincides with the slip direction. It is approximate in other cases. The analysis shows that dislocation emission is controlled by the unstable stacking energy γ_{us} . This parameter corresponds to the maximum energy experienced by slipping one half of a crystal rigidly with respect the other half along the Burgers vector of the emitted dislocation. It is thus closely related to the generalized stacking fault (GSF) surface introduced by Vitek (1968) which

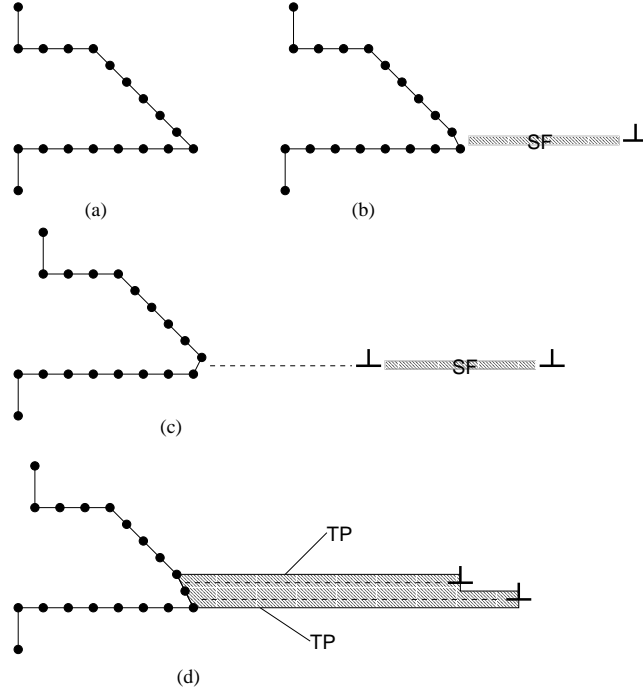


Fig. 2. Schematic representation of dissociated dislocation nucleation versus deformation twinning at a crack tip (only the crack tip atoms are drawn). Frame (a) shows the undisturbed crack tip. In frame (b) a leading partial dislocation has been emitted from the crack tip leaving behind a stacking fault. In frame (c) a dissociated dislocation has been formed by the emission of the trailing partial. In frame (d) a microtwin has been nucleated by the emission of another leading partial dislocation on a parallel slip plane. “SF” indicates an intrinsic stacking fault and “TP” a twin plane. The figure is drawn for an fcc material with a $\{111\}$ crack plane and a $\langle 110 \rangle$ crack direction with the crack terminated by a $\{001\}$ plane. This will later be referred to as the sharp crack tip morphology.

maps the interplanar energy across the entire slip plane.

In his analysis, Rice explicitly considers the nucleation of dissociated dislocations which are formed in two steps, as shown in Fig. 2 for the special case where the slip plane is coincident with the crack plane. First, a leading partial dislocation is emitted from the crack tip leaving an intrinsic stacking fault ribbon in its wake (frames a and b). Second, the trailing partial dislocation is emitted on the same slip plane completing the dissociated dislocation (frame c) which is then free to move away from the crack tip. In this paper we consider an alternative to the above scenario. If instead of the emission of the trailing partial, a second leading partial is nucleated on the slip plane above the original emission plane (frame d), then a two-layer thick *microtwin* is nucleated instead of a dissociated dislocation. The microtwin is bounded on the top and bottom by twin planes and on the sides by the crack tip and the partial dislocations. An intrinsic stacking fault exists between the two partials and an extrinsic stacking fault exists between the second partial and the crack tip.

The microtwin cannot be considered a true twin due to the interaction of the twin planes across the extrinsic stacking fault. The energy of these boundaries will generally be higher than that of true twin boundaries. Despite this we refer to the defect as a microtwin for two reasons: (1) the morphology of the defect which is bounded by twin planes and terminated by the leading partials at an incoherent interface is characteristic of twins; and (2) atomistic simulations (Hai and Tadmor, 2003) have shown that in all cases, once a microtwin has formed at a crack tip, increasing the load causes it to thicken into a true twin. The microtwin may then be considered a precursor to DT and a criterion for its appearance is thus also a criterion for the initiation of twinning at a crack tip. In the remainder of the paper whenever nucleation of a twin is discussed it is to be understood that the meaning is the nucleation of a microtwin. In addition, the leading partial leading to the formation of the microtwin will sometimes be referred to as the twinning partial.

A criterion for the nucleation of a deformation twin can be formulated in terms of the competition between the nucleation of the trailing partial needed to complete the dissociated dislocation and the nucleation of the twinning partial needed to form the microtwin. The analysis for the emission of the twinning partial is based on the Peierls concept, as is the Rice criterion for dislocation emission, and is derived in a similar manner. The main difference is that the GSF surface used to characterize the energetics of the interplanar potential must account for the fact that an intrinsic stacking fault now exists in the crystal. Similar to Rice's criterion, the emission of the twinning partial is found to be controlled by the maximum energy encountered when slipping along the Burgers vector of the twinning partial. However, this value is no longer γ_{us} but rather a new material parameter γ_{ut} , which we name the *unstable twinning energy* in analogy to the Rice parameter. We will see that γ_{ut} plays the same role for DT as γ_{us} does for dislocation emission.

We now turn to the derivation of the nucleation criteria. We begin by deriving the criterion for the special case where the slip plane ahead of the crack tip is coplanar with the crack plane. The case of an inclined slip plane, where additional approximations must be made, is treated afterwards. No particular crystal structure is assumed in the derivation. The fcc lattice is used as a specific example in some places to help clarify certain aspects of the derivation.

2.2 DT criterion for coplanar slip and crack planes

In this section we derive the twinning criterion for the case where the slip plane ahead of the crack tip is coplanar with the crack plane and the loading and slip directions are arbitrary. Referring to Fig. 1 this corresponds to the case where $\theta = 0$, the SIF's are K_I , K_{II} and K_{III} and the partial dislocation slip

directions are ϕ_A and ϕ_B . Rice's results for the critical SIF's for the emission of the leading and trailing partials are given without derivation. The reader is referred to Rice (1992) for a more complete discussion.

Emission of the leading partial

The problem is solved through application of the J-Integral (Rice, 1968). A displacement discontinuity $\boldsymbol{\delta} = \mathbf{u}^+ - \mathbf{u}^-$ is taken to exist along the x_1 -axis ahead of the crack tip (Fig. 1), where \mathbf{u} is the displacement field. It is assumed that the discontinuity has the form $\boldsymbol{\delta} = \delta(\cos \phi_A \mathbf{e}_1 + \sin \phi_A \mathbf{e}_3) = \delta \mathbf{e}_A$, where shear-tension coupling is neglected ($\delta_2 = 0$) and slip is constrained to the leading partial direction. Applying the Peierls concept, the shear stress along the x_1 -axis is taken to be a function of the local slip discontinuity, $\tau(x_1) = f(\delta(x_1))$. The stress may be obtained from a corresponding interplanar potential $\Phi(\boldsymbol{\delta})$ by differentiation. For slip along the leading partial direction, we define the one-dimensional (1D) potential,

$$\Phi_A(\delta) \equiv \Phi(\delta \mathbf{e}_A) = \Phi(\delta \cos \phi_A, 0, \delta \sin \phi_A). \quad (1)$$

The shear stress along the slip direction is then given by

$$\tau_A = \frac{d\Phi_A}{d\delta} = \frac{\partial \Phi}{\partial \delta_1} \cos \phi_A + \frac{\partial \Phi}{\partial \delta_3} \sin \phi_A = \sigma_{21} \cos \phi_A + \sigma_{23} \sin \phi_A. \quad (2)$$

Away from the slip plane the material is assumed to be linear elastic and isotropic with shear modulus μ and Poisson's ratio ν .

Rice (1992) pointed out that the potential $\Phi(\boldsymbol{\delta})$ used in the Peierls model is related (but not equal) to the GSF interplanar potential $\Psi(\boldsymbol{\Delta})$. The difference is that $\Psi(\boldsymbol{\Delta})$ is the energy obtained by rigidly displacing one half of a crystal relative to the other, where $\boldsymbol{\Delta}$ is the disregistry of atoms across the cut plane. For a lattice undergoing a uniform shear $\boldsymbol{\gamma} = \gamma_1 \mathbf{e}_1 + \gamma_3 \mathbf{e}_3$ outside of the slip plane, the disregistry and slip discontinuity are related by $\boldsymbol{\Delta} = \boldsymbol{\delta} + \boldsymbol{\gamma}h$, where h is the interplanar spacing normal to the slip plane. It may be shown that $\Phi(\boldsymbol{\delta})$ and $\Psi(\boldsymbol{\Delta})$ are related according to $\Phi = \Psi - h(\sigma_{21}^2 + \sigma_{23}^2)/2\mu$. An important consequence of this relation is that $\Phi(\boldsymbol{\delta})$ and $\Psi(\boldsymbol{\Delta})$ share the same extrema. In particular, the parameter γ_{us} , a maximum on the $\Phi(\boldsymbol{\delta})$ surface which plays an important role in the nucleation criterion, may be obtained directly from the corresponding $\Psi(\boldsymbol{\Delta})$ function. This is advantageous because the GSF potential may be readily calculated using atomistic techniques.

The nucleation problem was solved by Rice (1992) by utilizing the path invariance property of the J-integral. By evaluating J in the far field where the stress field is characterized by the applied SIF's and comparing this with J

evaluated on the slip plane where the shear stress is given by (2), the following relation is obtained,

$$\frac{(1 - \nu)K_A^2/2\mu}{\cos^2 \phi_A + (1 - \nu) \sin^2 \phi_A} = \Phi_A(\delta_{\text{tip}}), \quad (3)$$

where

$$K_A = \cos \phi_A K_{\text{II}} + \sin \phi_A K_{\text{III}}, \quad (4)$$

is the intensity factor for the shear stress along the slip direction and $\Phi_A(\delta_{\text{tip}})$ is the value of the interplanar potential at the crack tip.

As K_A increases with the external loading, the energy stored in the slipped zone increases and the potential at the crack tip follows the $\Phi_A(\delta)$ curve. At the first maximum, the system loses stability and a partial dislocation is emitted. This maximum is defined as the unstable stacking energy γ_{us} . The critical SIF for the nucleation of the leading partial is thus,

$$K_{\text{Acrit}} \equiv \sqrt{\frac{2\mu}{1 - \nu} [\cos^2 \phi_A + (1 - \nu) \sin^2 \phi_A] \gamma_{\text{us}}}. \quad (5)$$

The sequence of events associated with the nucleation of the partial is demonstrated in Fig. 3, where the solid line connecting points I and III corresponds to the GSF potential $\Psi(\Delta)$ for slip along the leading partial direction. The system will lose stability at point II, where $\Phi_A(\delta_{\text{tip}}) = \Psi(\Delta_{\text{tip}} \mathbf{e}_A) = \gamma_{\text{us}}$, and emit a partial dislocation. Following the emission, the slip plane behind the partial contains an intrinsic stacking fault and remains at an elevated energy level γ_{sf} (point III). The slip at this point is equal to the magnitude of the Burgers vector of the leading partial b_A (in an fcc crystal, $b_A = a_0/\sqrt{6}$ where a_0 is that lattice parameter). The atomic configurations associated with the extrema I, II and III through which the system passes during the emission of the leading partial are displayed below the curves. The curves in Fig. 3 were computed using an embedded atom method (EAM) (Daw and Baskes, 1983) potential for aluminum due to Ercolessi and Adams (1993).

The nucleated partial dislocation will move away from the crack tip and settle at an equilibrium distance r_A . This distance is determined by the balance of image and stacking fault forces drawing the dislocation back to the crack tip and the Peach-Koehler force driving the dislocation away,

$$K_A b_A / \sqrt{2\pi r_A} = \gamma_{\text{sf}} + \mu b_A^2 [\cos^2 \phi_A + (1 - \nu) \sin^2 \phi_A] / 4\pi(1 - \nu)r_A. \quad (6)$$

The equilibrium equation in (6) has two roots: a point of unstable equilibrium

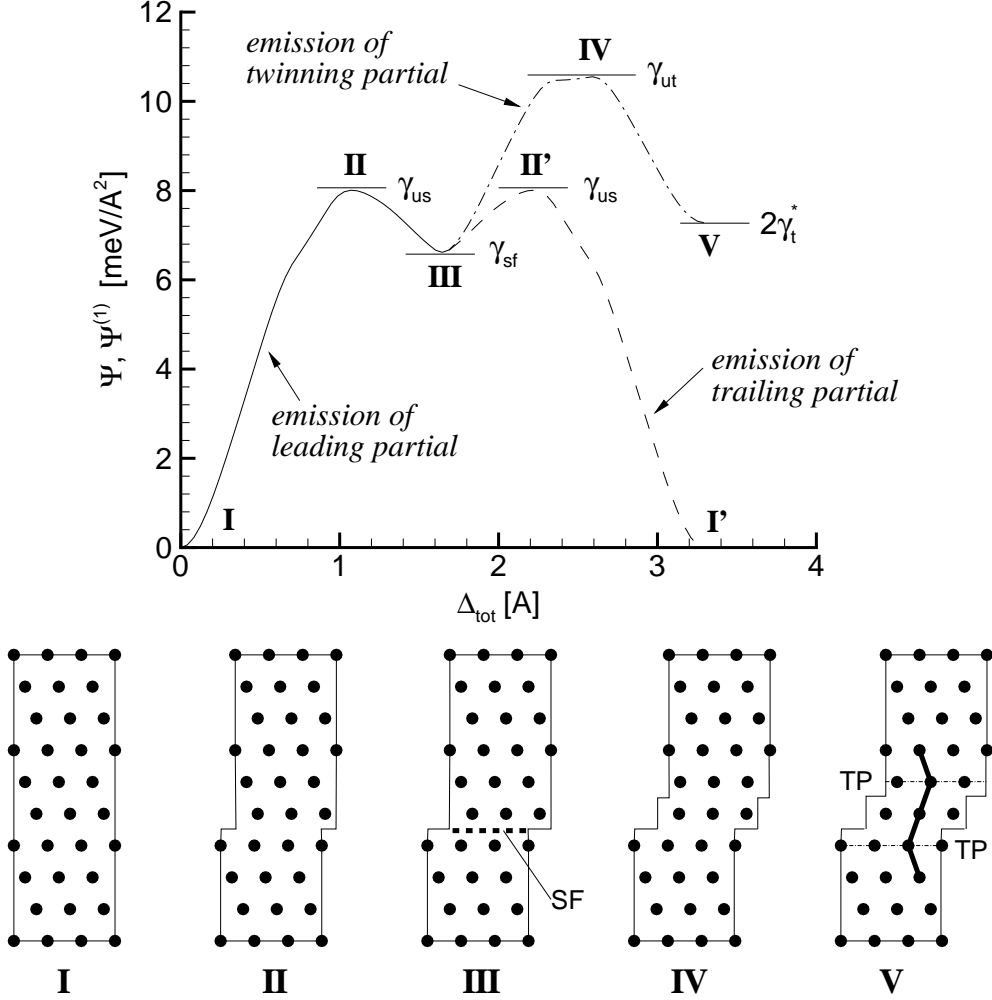


Fig. 3. The interplanar potentials for aluminum and associated atomic configurations. The figure contains three curves: (1) The solid line is the GSF potential $\Psi(\Delta)$ for slip along the leading partial direction, $\Delta = \Delta_{\text{tot}}\mathbf{e}_A$. (2) The dashed line corresponds to $\Psi(\Delta)$ for slip along the trailing partial direction after the emission of the leading partial, $\Delta = b_A\mathbf{e}_A + (\Delta_{\text{tot}} - b_A)\mathbf{e}_B$, where for aluminum $b_A = 1.646\text{\AA}$. (3) The dash-dot line corresponds to the faulted potential $\Psi^{(1)}(\Delta)$ for a crystal containing an intrinsic stacking fault. The curve is plotted for slip along the leading partial direction, $\Delta = (\Delta_{\text{tot}} - b_A)\mathbf{e}_A$. For curves (2) and (3), Δ_{tot} is the total slip including that of the leading partial. The atomic configurations associated with the labeled extrema on the curves are displayed below them. “SF” indicates an intrinsic stacking fault and “TP” a twin plane.

very close to the origin and a point of stable equilibrium normally at $r_A \gg b_A$. The larger root is the one of interest,

$$r_A = \frac{K_A^2 b_A^2}{8\pi\gamma_{sf}^2} \left[1 + \sqrt{1 - \frac{\gamma_{sf}}{\gamma_{us}} \left(\frac{K_{Acrit}}{K_A} \right)^2} \right]^2. \quad (7)$$

A related identity which will be useful later is

$$\frac{\mu b_A}{(1-\nu)\sqrt{2\pi r_A}} = \frac{K_A [1 - \sqrt{1 - (\gamma_{sf}/\gamma_{us})(K_{Acrit}/K_A)^2}]}{\cos^2 \phi_A + (1-\nu) \sin^2 \phi_A}. \quad (8)$$

Emission of the trailing partial

As the external loading continues to increase the incipient slip associated with the trailing partial may begin to form. The critical SIF for the emission of the trailing partial is obtained in a similar manner to the emission of the leading partial. There are, however, several important differences:

- (i) The leading partial dislocation that was emitted earlier shields the crack tip and reduces the crack tip SIF's to K_{II}^* and K_{III}^* ,

$$K_{II}^* = K_{II} - \frac{\mu b_A}{(1-\nu)\sqrt{2\pi r_A}} \cos \phi_A, \quad K_{III}^* = K_{III} - \frac{\mu b_A}{\sqrt{2\pi r_A}} \sin \phi_A. \quad (9)$$

- (ii) The slip direction associated with the trailing partial is ϕ_B .
- (iii) The interplanar potential characterizing the constitutive response along the new slip direction must account for the prior emission of the leading partial dislocation. The 1D potential used in the analysis is thus

$$\Phi_B(\delta) = \Phi(b_A \mathbf{e}_A + \delta \mathbf{e}_B), \quad (10)$$

where $\mathbf{e}_B = \cos \phi_B \mathbf{e}_1 + \sin \phi_B \mathbf{e}_3$.

Subject to the conditions listed above, the results in the previous section are rederived, leading to a relation analogous to (3),

$$\frac{(1-\nu)K_B^{*2}/2\mu}{\cos^2 \phi_B + (1-\nu) \sin^2 \phi_B} = \Phi_B(\delta_{tip}) - \Phi_B(0), \quad (11)$$

where

$$K_B^* = \cos \phi_B K_{II}^* + \sin \phi_B K_{III}^*. \quad (12)$$

The nucleation criterion will be associated with extrema of the interplanar potential. To clarify this we refer again to Fig. 3, where the dashed line corresponds to the energy associated with slip along the trailing partial direction. Slip now begins at point III where the leading partial nucleation ended. The ground level energy associated with zero slip is not zero as it was for the leading partial emission. Instead, $\Phi_B(0) = \Phi(b_A \mathbf{e}_A) = \Phi_A(b_A) = \gamma_{sf}$. The system will lose stability when $\Phi_B(\delta_{tip})$ reaches a first maximum. This occurs at point II' where the energy is γ_{us} . At the end of the emission the slip plane behind the resulting dissociated dislocation is undisturbed with zero energy penalty (point I'). Given the above, the nucleation criterion for the trailing partial is obtained from (11) as

$$K_B^* = \sqrt{\frac{2\mu}{1-\nu} [\cos^2 \phi_B + (1-\nu) \sin^2 \phi_B]} (\gamma_{us} - \gamma_{sf}) \equiv K_{Bcrit}^*, \quad (13)$$

where K_{Bcrit}^* has been defined as the critical shielded SIF for emission of the trailing partial. Substituting (9) into (12) and making use of (8), the following explicit expression is obtained for K_B^* ,

$$K_B^* = K_B - \eta K_A + \eta \sqrt{K_A^2 - \frac{2\mu}{1-\nu} [\cos^2 \phi_A + (1-\nu) \sin^2 \phi_A] \gamma_{sf}}, \quad (14)$$

where

$$K_B = \cos \phi_B K_{II} + \sin \phi_B K_{III}, \quad (15)$$

$$\eta = \frac{\cos \phi_A \cos \phi_B + (1-\nu) \sin \phi_A \sin \phi_B}{\cos^2 \phi_A + (1-\nu) \sin^2 \phi_A}. \quad (16)$$

Emission of the twinning partial

Once the leading partial dislocation has been emitted (and before the emission of the trailing partial), a competition exists between two possible modes of deformation. The system will either nucleate the trailing partial of the dissociated dislocation or nucleate another partial dislocation of the leading type on an adjacent plane forming a microtwin (Fig. 2). To quantify this competition, the critical SIF required to nucleate the twinning partial needs to be computed and compared to the trailing partial nucleation criterion in (13). Since the nucleation of the microtwin involves the emission of a partial dislocation, exactly as in the previous cases, a Peierls analysis may be applied here as well. The derivation in this case closely follows the derivation for the trailing partial, detailed in the previous section, with two main exceptions: (1) The twinning partial dislocation has the same orientation as the leading

partial, so $\phi_B = \phi_A$; and (2) a different interplanar potential must be used as explained below.

The interplanar potential $\Phi(\boldsymbol{\delta})$ used in the analyses for the emission of the leading and trailing partials is defined for a slip discontinuity introduced between two otherwise perfect crystal halves. This is not the case for the slip formed during the nucleation of the twinning partial. This partial is emitted on a plane adjacent to the plane where the leading partial was emitted and formed an intrinsic stacking fault. To account for this, the interplanar potential has to be generalized to crystals deformed by the passage of partial dislocations. In general, we define $\Phi^{(i)}(\boldsymbol{\delta})$ as the faulted interplanar potential for a crystal where i partial dislocation have passed on adjacent planes. $\Phi^{(1)}(\boldsymbol{\delta})$ corresponds to a crystal with an intrinsic stacking fault, $\Phi^{(2)}(\boldsymbol{\delta})$ to a crystal with an extrinsic stacking fault, $\Phi^{(3)}(\boldsymbol{\delta})$ to a crystal with a three-layer twin, and so on. The slip discontinuity is introduced on one of the planes adjacent to the faulted region. For the emission of the twinning partial, $\Phi^{(1)}(\boldsymbol{\delta})$ is the appropriate potential. The twinning partial is formed by slip along the leading partial direction ϕ_A and so the corresponding 1D potential used in the analysis is

$$\Phi_A^{(1)}(\delta) = \Phi^{(1)}(\delta \mathbf{e}_A). \quad (17)$$

Associated with the faulted interplanar potentials is a family of faulted GSF potentials $\Psi^{(i)}(\boldsymbol{\Delta})$. These functions map the interplanar energy of a crystal containing a faulted region i -layers thick (as explained above), when the part of the crystal one layer above the faulted region is rigidly displaced relative to the rest of the crystal. This is demonstrated in Fig. 3, where the dash-dot line corresponds to the $\Psi^{(1)}(\boldsymbol{\Delta})$ potential for slip along the leading partial direction. Slip begins at point III where $\Psi^{(1)}(0) = \gamma_{\text{sf}}$ (in the figure the curve has been shifted to the right to join up with the $\Psi(\boldsymbol{\Delta})$ curve). As slip increases a maximum is encountered at point IV. This maximum is the unstable twinning energy γ_{ut} . The interplanar energy reaches a new minimum at point V following the application of a full Burgers vector of slip. At this point an extrinsic stacking fault bounded by two twin planes has been formed. The energy of the fault is $2\gamma_t^*$ where γ_t^* is nearly equal to the true twin boundary energy γ_t except for distant-neighbor interaction effects. The atomic configurations associated with points IV and V are displayed below the curves. As before, the extrema of the interplanar potential play an important role in the derivation of the critical SIF.

The derivation leads to the following relation analogous to (3) and (11),

$$\frac{(1 - \nu)K_A^{*2}/2\mu}{\cos^2 \phi_A + (1 - \nu) \sin^2 \phi_A} = \Phi_A^{(1)}(\delta_{\text{tip}}) - \Phi_A^{(1)}(0), \quad (18)$$

where

$$K_A^* = \cos \phi_A K_{\text{II}}^* + \sin \phi_A K_{\text{III}}^*. \quad (19)$$

Referring to the extrema of the $\Psi^{(1)}(\Delta)$ curve, we note that $\Phi_A^{(1)}(0) = \gamma_{\text{sf}}$ and $\Phi_A^{(1)}(\delta_{\text{tip}}) = \gamma_{\text{ut}}$ at the first maximum. The nucleation criterion then follows from (18) as

$$K_A^* = \sqrt{\frac{2\mu}{1-\nu} [\cos^2 \phi_A + (1-\nu) \sin^2 \phi_A]} (\gamma_{\text{ut}} - \gamma_{\text{sf}}) \equiv K_{\text{Acrit}}^*, \quad (20)$$

where K_{Acrit}^* is the critical shielded SIF for emission of the twinning partial dislocation. Substituting (9) into (19) and making use of (8) and (5) gives

$$K_A^* = \sqrt{K_A^2 - \frac{2\mu}{1-\nu} [\cos^2 \phi_A + (1-\nu) \sin^2 \phi_A]} \gamma_{\text{sf}}. \quad (21)$$

Substituting (21) into (20), the criterion for the emission of the twinning partial is obtained in the simple form,

$$K_A = \sqrt{\frac{2\mu}{1-\nu} [\cos^2 \phi_A + (1-\nu) \sin^2 \phi_A]} \gamma_{\text{ut}} \equiv K_{\text{Acrit}}^T, \quad (22)$$

where K_{Acrit}^T is defined as the critical resolved SIF for nucleation of the twinning partial. Comparing this expression to (5) we see that γ_{ut} plays the same role for DT as γ_{us} does for dislocation emission. In the analysis that follows we will see that the unstable twinning energy plays a key role in determining the propensity of a material to twin.

Twinning criterion

The nucleation criteria in (13) and (22) for the trailing and twinning partials, assume that K_{II} and K_{III} are independent. This makes interpretation of the results difficult. It is also not possible to define a twinning criterion in a simple fashion. As the external loading is increased, the crack tip will either emit a dislocation or twin depending on which nucleation criterion is satisfied first. A twinning criterion may be defined, however, by limiting the discussion to the case where K_{II} and K_{III} are not independent, but are the components of a mixed-mode SIF K acting at some fixed angle α ,

$$K_{\text{II}} = K \cos \alpha, \quad K_{\text{III}} = K \sin \alpha. \quad (23)$$

This is a special case, but an important one since in many cases there is a single external load applied to the system with other loads proportional to it. Substituting (23) into (4) and (15) gives,

$$K_A = K \cos(\phi_A - \alpha), \quad K_B = K \cos(\phi_B - \alpha). \quad (24)$$

The dislocation emission criteria may now be rewritten in a simpler form. The criterion for the emission of the leading partial in terms of K is,

$$K = K_{A\text{crit}} / \cos(\phi_A - \alpha) \equiv K^1, \quad (25)$$

where $K_{A\text{crit}}$ is given in (5). The criterion for the emission of the trailing partial in terms of K can be shown to be,

$$(r - \eta)K + \eta\sqrt{K^2 - g(K^1)^2} = K_{B\text{crit}}^* / \cos(\phi_A - \alpha), \quad (26)$$

where $r = \cos(\phi_B - \alpha) / \cos(\phi_A - \alpha)$, $g = \gamma_{\text{sf}} / \gamma_{\text{us}}$, K^1 is defined in (25), and $K_{B\text{crit}}^*$ is defined in (13). Equation (26) may be further simplified by setting $K = \lambda K^1$, where λ is a dimensionless factor, and dividing through by K^1 ,

$$(r - \eta)\lambda + \eta\sqrt{\lambda^2 - g} = \kappa, \quad (27)$$

where $\kappa = K_{B\text{crit}}^* / K_{A\text{crit}}$. Equation (27) needs to be checked for spontaneous emission of the trailing partial dislocation. This occurs if the left-hand side of the equation is greater than the right-hand side for $\lambda = 1$,

$$r - \eta + \eta\sqrt{1 - g} \geq \kappa. \quad (28)$$

If condition (28) is not satisfied then equation (27) may be rearranged to yield the following quadratic equation for the critical λ necessary to emit the trailing partial,

$$r(2\eta - r)\lambda^2 - 2(\eta - r)\kappa\lambda - (\kappa^2 + g\eta^2) = 0. \quad (29)$$

Relevant solutions will be greater than one. For fcc materials it may be shown that this condition is only satisfied by the positive root,

$$\lambda_{\text{crit}} = \frac{(\eta - r)\kappa + \eta\sqrt{\kappa^2 + gr(2\eta - r)}}{r(2\eta - r)}. \quad (30)$$

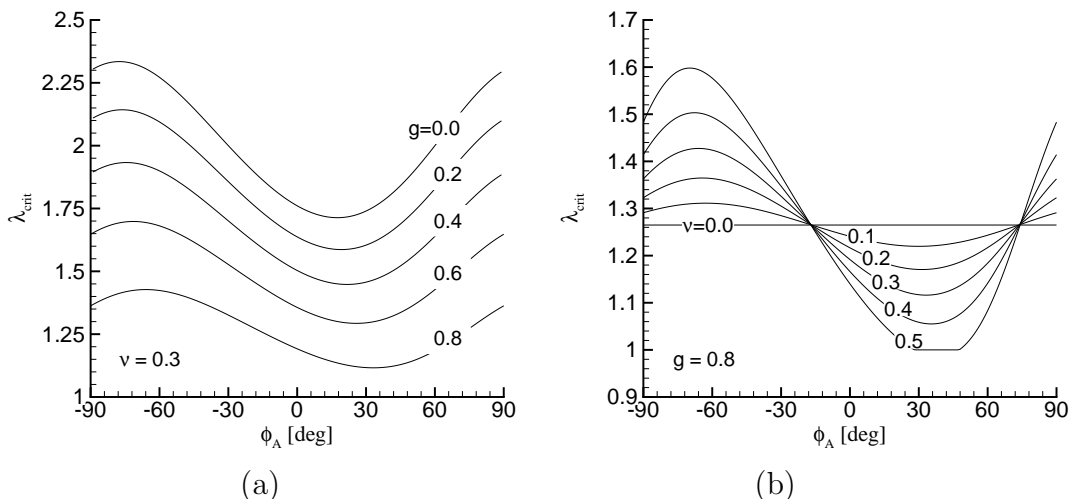


Fig. 4. Critical normalized nucleation load λ_{crit} of the trailing partial dislocation as a function of the leading partial direction ϕ_A . Curves are plotted for an fcc material with the load direction coincident with the leading partial direction. Frame (a) shows the dependence of λ_{crit} on $g = \gamma_{\text{sf}}/\gamma_{\text{us}}$ for $\nu = 0.3$. Frame(b) shows the dependence on ν for $g = 0.8$.

The nucleation criterion for the trailing partial can now be written explicitly in terms of K ,

$$K = \lambda_{\text{crit}} K^1 \equiv K^\perp. \quad (31)$$

The normalized nucleation load λ_{crit} depends on the material parameters γ_{sf} , γ_{us} (through the ratio g) and ν (but not μ), and the geometric parameters α , ϕ_A and ϕ_B . It is of interest to study the dependence of λ_{crit} on these parameters. Figs. 4(a) and 4(b) present a parametric study of the dependence of λ_{crit} on $g = \gamma_{\text{sf}}/\gamma_{\text{us}}$ and ν in fcc materials. For fcc, $\Delta\phi \equiv \phi_B - \phi_A = \pm 60^\circ$.¹ The curves are drawn for the case where the loading direction coincides with the leading partial direction ($\alpha = \phi_A$). For $\alpha > \phi_A$, λ_{crit} is lower and in most cases spontaneous emission of the trailing partial is predicted at the maximum value of α ($\alpha_{\text{max}} = \phi_A + \Delta\phi/2$).² The curves are thus an upper bound on the emission load. In Fig. 4(a) we see that nucleation of the trailing partial requires a larger load for lower values of g , i.e. for cases where the stacking fault energy is lower relative to the unstable stacking energy. This result is not immediately obvious since reducing γ_{sf} affects λ_{crit} in two opposite ways: (1) For lower values of γ_{sf} the equilibrium distance of the leading partial is greater and hence the shielding of the crack tip is lower, which tends to reduce the necessary nucleation load; (2) For lower values of γ_{sf} the barrier for emitting

¹ The curves in figure 4 are drawn for $\Delta\phi = 60^\circ$. For $\Delta\phi = -60^\circ$ a mirror image of the curves relative to $\phi_A = 0$ is obtained.

² For $\alpha > \alpha_{\text{max}}$, B would become the leading partial in place of A.

the trailing partial increases, which tends to increase the nucleation load. Fig. 4(a) shows that the second effect dominates the behavior of the system. In Fig. 4(b) we see that the effect of ν on the nucleation load depends on the angle of the leading partial direction. For $\phi_A < -17^\circ$ increasing ν increases the nucleation load. For $\phi_A > -17^\circ$ the effect is reversed.

Returning to the twinning criterion, the expression for the nucleation of the twinning partial in terms of K is,

$$K = K_{Acrit}^T / \cos(\phi_A - \alpha) \equiv K^T, \quad (32)$$

where K_{Acrit}^T is defined in (22). We define the *twinning tendency* of a material T as the ratio of the SIF necessary to nucleate the trailing partial and that necessary to nucleate the twinning partial. A microtwin will nucleate when $T > 1$ and a dislocation when $T < 1$. This is the twinning criterion. After some manipulation, T takes on the particularly simple form,

$$T \equiv \frac{K^\perp}{K^T} = \lambda_{crit} \sqrt{\frac{\gamma_{us}}{\gamma_{ut}}}. \quad (33)$$

The twinning tendency expression in (33) lends itself to a clear physical explanation. We see that T is affected by two factors: λ_{crit} , which characterizes the additional load necessary to nucleate the trailing partial relative to the leading partial, and γ_{us}/γ_{ut} , the ratio of the energy barriers for dislocation emission and DT. For cases where spontaneous emission of the trailing partial does not occur, λ_{crit} will be larger than one. The larger the value of λ_{crit} the larger that of T , signifying that DT is becoming more favorable due to the difficulty in nucleating the trailing partial. The ratio γ_{us}/γ_{ut} will normally be less than one, so this factor tends to reduce T . In particular, the larger the value of γ_{ut} the more difficult it is for the material to twin. For cases where spontaneous emission of the trailing partial occurs, λ_{crit} will be less than one and hence T will also be less than one. The twinning criterion will thus predict dislocation emission in this case, consistent with the behavior of the system. In section 3, a detailed analysis of the predictions of the criterion is given for the systems studied in the atomistic simulations of Hai and Tadmor (2003).

2.3 DT criterion for arbitrary slip plane inclination

In this section we consider the general case where the slip plane may be inclined with respect to the crack plane ($\theta \neq 0$) along with arbitrary loading and partial dislocation directions. We treat this case in an approximate fashion following the suggestion in Rice (1992) to define effective mode II and III SIF's on the

inclined plane as,

$$K_{\text{II}}^{\text{eff}} = K_{\text{I}}f_{\text{I}}(\theta) + K_{\text{II}}f_{\text{II}}(\theta), \quad K_{\text{III}}^{\text{eff}} = K_{\text{III}}f_{\text{III}}(\theta), \quad (34)$$

where

$$f_{\text{I}}(\theta) = \cos^2 \frac{\theta}{2} \sin \frac{\theta}{2}, \quad f_{\text{II}}(\theta) = \cos \frac{\theta}{2} [1 - 3 \sin^2 \frac{\theta}{2}], \quad f_{\text{III}}(\theta) = \cos \frac{\theta}{2}. \quad (35)$$

The expressions derived in the previous section for the emission of the leading partial (5), trailing partial (13) and twinning partial (22) may then be used with K_{II} and K_{III} replaced by $K_{\text{II}}^{\text{eff}}$ and $K_{\text{III}}^{\text{eff}}$. The fundamental assumption here is that a dislocation or a microtwin will nucleate on an inclined plane when the resolved shear stresses on that plane are the same as those that would cause the defect to nucleate on a slip plane coincident with the crack plane with the same slip directions. This is clearly an approximation.

It is not possible to define the twinning tendency for this general case since there are more than one independent loads. To determine whether DT or dislocation emission occurs, it is necessary to define a loading regime and then gradually increase the loads, checking conditions (13) and (22) along the way. The first condition to be satisfied will determine the resulting mode of deformation. There are two interesting special cases where it is possible to define the twinning tendency and hence to obtain an explicit criterion for DT. These are the cases of pure mode I loading and mixed mode II and III loading with a fixed loading angle α as defined in (23). For pure mode I loading, $K_{\text{II}}^{\text{eff}} = K_{\text{I}} \cos^2(\theta/2) \sin(\theta/2)$ and $K_{\text{III}}^{\text{eff}} = 0$, which corresponds to the solution in the previous section with $K = K_{\text{I}} \cos^2(\theta/2) \sin(\theta/2)$ and $\alpha = 0$. The trailing partial will nucleate according to (31) when,

$$K_{\text{I}} = K^{\perp} / \cos^2(\theta/2) \sin(\theta/2). \quad (36)$$

The twinning partial will nucleate according to (32) when,

$$K_{\text{I}} = K^T / \cos^2(\theta/2) \sin(\theta/2). \quad (37)$$

While the inclination of the slip plane θ clearly affects the absolute magnitude of the emission loads in the above expressions, interestingly the twinning tendency, which is defined as a ratio of these loads, is not affected. Thus the twinning criterion for pure mode I loading depends only on material parameters and the slip directions and not on the slip plane angle θ .

For mixed mode II and III loading, the effective SIF's are,

$$K_{\text{II}}^{\text{eff}} = K \cos \alpha \cos \frac{\theta}{2} (1 - 3 \sin^2 \frac{\theta}{2}), \quad K_{\text{III}}^{\text{eff}} = K \sin \alpha \cos \frac{\theta}{2}. \quad (38)$$

It is not possible to define an effective angle α linking $K_{\text{II}}^{\text{eff}}$ and $K_{\text{III}}^{\text{eff}}$. Instead the resolved SIF's K_A and K_B are given by $K_A = c_A K$ and $K_B = c_B K$, where

$$c_A = \cos(\theta/2) [\cos(\phi_A - \alpha) - 1.5 \cos \alpha \cos \phi_A (1 - \cos \theta)], \quad (39)$$

$$c_B = \cos(\theta/2) [\cos(\phi_B - \alpha) - 1.5 \cos \alpha \cos \phi_B (1 - \cos \theta)]. \quad (40)$$

The leading partial dislocation will nucleate when,

$$K = K_{A\text{crit}}/c_A \equiv K_{\text{eff}}^1. \quad (41)$$

A special case exists when $c_A = 0$. In this case $K_A = 0$ and A is not a possible leading partial direction. The trailing partial dislocation will nucleate when,

$$K = \lambda_{\text{crit}} K_{\text{eff}}^1 \equiv K_{\text{eff}}^\perp, \quad (42)$$

where λ_{crit} is given by (30), but with $r = c_B/c_A$. The twinning partial will nucleate when,

$$K = K_{A\text{crit}}^T/c_A \equiv K_{\text{eff}}^T. \quad (43)$$

The twinning tendency is given by (33).

2.4 Calculation of material parameters for several fcc materials

The critical SIF's for the emission of a dislocation or nucleation of a microtwin depend on the elastic constants of the material μ and ν and the three energy parameters γ_{sf} , γ_{us} and γ_{ut} . Experimental values are readily available for the elastic constants. Experimental values for intrinsic stacking fault energies can be obtained indirectly, for example by measuring the splitting distance of a dissociated dislocation. The difficulty is posed by the nucleation barriers γ_{us} and γ_{ut} for which independent experimental measurements are difficult if not impossible. An alternative is to calculate these parameters directly using atomistic techniques.

As a first estimate for the value of γ_{ut} , we carried out atomistic calculations using empirical EAM potentials. Many EAM potentials tend to grossly underestimate stacking fault energies making their predictions for γ_{us} and γ_{ut}

Mat	γ_{us}	γ_{sf}	γ_{ut}	$2\gamma_{\text{t}}^*$	$\gamma_{\text{ut}2}$	$2\gamma_{\text{t}}$	$\gamma_{\text{sf}}/\gamma_{\text{us}}$	$\gamma_{\text{us}}/\gamma_{\text{ut}}$
Al	8.007	6.616	10.55	7.280	10.66	7.261	0.826	0.756
Ag	5.683	0.907	6.148	0.932	6.145	0.931	0.160	0.924
Cu	9.269	2.260	10.37	2.275	10.38	2.274	0.244	0.894

Table 1

GSF surface energies for different materials. All energies are given in $\text{meV}/\text{\AA}^2$. In addition the dimensionless ratios $\gamma_{\text{sf}}/\gamma_{\text{us}}$ and $\gamma_{\text{us}}/\gamma_{\text{ut}}$ on which the twinning criterion depends are given.

suspect. In this section we present results for three EAM potentials for which the stacking fault energies are in reasonable agreement with experimental values. These are the Ercolessi and Adams (1993) potential for aluminum and the Voter (1994) potentials for silver and copper. The results for the Ercolessi and Adams potential are of particular interest because in the next section the predictions of the theoretical model are compared with atomistic simulations of crack tip deformation that were performed using this potential. The energy parameters computed for the three potentials are given in Table 1. The calculations were carried out using a supercell containing two of the interfaces being evaluated. Periodic boundary conditions were applied in all three directions. The distance between the interfaces was increased (by extending the supercell in the z -direction normal to the interfaces) until the interfacial energy was independent of the separation. Relaxation of the atomic layers in the z -direction and uniform expansion/contraction of the supercell in the same direction were enabled. For each potential Table 1 lists γ_{sf} , γ_{us} and γ_{ut} along with three additional energy parameters: the extrinsic stacking fault energy $2\gamma_{\text{t}}^*$; the parameter $\gamma_{\text{ut}2}$ which is the barrier for the emission of the third partial resulting in the formation of a true twin ($\gamma_{\text{ut}2}$ is a maximum on the $\Psi^{(2)}(\Delta)$ surface); and twice the twin boundary energy $2\gamma_{\text{t}}$. The parameters are listed in the order they would be experienced as partials nucleate and propagate on adjacent planes (Fig. 3). As mentioned above, the EAM values should only be considered a first estimate. *Ab initio* quantum mechanical calculations for the stacking fault and twin boundary energies in aluminum (Hammer et al., 1992) give $\gamma_{\text{sf}}=9.75 \text{ meV}/\text{\AA}^2$, $2\gamma_{\text{t}}^*=8.63 \text{ meV}/\text{\AA}^2$ and $2\gamma_{\text{t}}=7.50 \text{ meV}/\text{\AA}^2$. By comparison the EAM values are too low and their ordering is incorrect. For the EAM potential $\gamma_{\text{sf}} < 2\gamma_{\text{t}}^* \approx 2\gamma_{\text{t}}$ whereas the *ab initio* values satisfy $\gamma_{\text{sf}} > 2\gamma_{\text{t}}^* > 2\gamma_{\text{t}}$. An *ab initio* calculation for the unstable stacking energy in aluminum (Lu et al., 2000) gives $\gamma_{\text{us}}=14 \text{ meV}/\text{\AA}^2$, almost double the EAM value. These discrepancies highlight the need for more accurate calculations for the unstable twinning energy γ_{ut} .

In addition to the energy parameters, Table 1 also includes the ratios $\gamma_{\text{sf}}/\gamma_{\text{us}}$ and $\gamma_{\text{us}}/\gamma_{\text{ut}}$ on which the twinning tendency (33) depends. The smaller the value of $\gamma_{\text{sf}}/\gamma_{\text{us}}$ and the larger the value of $\gamma_{\text{us}}/\gamma_{\text{ut}}$, the more likely a material is

Mat	c_{11}	c_{12}	c_{44}	μ	ν
Al	0.737	0.389	0.229	0.207	0.320
Ag	0.775	0.582	0.288	0.211	0.353
Cu	1.119	0.769	0.507	0.374	0.315

Table 2

Elastic constants and effective isotropic properties. Elastic constants c_{11} , c_{12} , c_{44} and μ are in unit of eV/Å³. Poisson's ration ν is dimensionless.

to twin (i.e. T becomes larger).³ We see that silver and copper have low values of $\gamma_{\text{sf}}/\gamma_{\text{us}}$ and high values of $\gamma_{\text{us}}/\gamma_{\text{ut}}$ relative to aluminum. Thus the criterion predicts that silver and copper should be more likely to twin than aluminum, in agreement with experimental results for these materials (Venables, 1963). The fact that the tendency of a material to twin increases with decreasing values of $\gamma_{\text{sf}}/\gamma_{\text{us}}$ is consistent with experimental findings that show that the twin nucleation stress decreases with decreasing values of the intrinsic stacking fault energy (Venables, 1963). However, these experimental results have led to the general belief that the tendency of a material to twin is primarily controlled by the intrinsic stacking fault energy, which the current model shows is only partly correct.

To complete the picture, Table 2 presents the elastic constants of the potentials considered as well as the effective isotropic constants μ and ν to be used with the theoretical model. The shear modulus and Poisson's ratio are taken to be the Voigt averages of the elastic constants (Hirth and Lothe, 1992),

$$\mu = \frac{1}{5}(c_{11} - c_{12} + 3c_{44}), \quad \nu = \frac{1}{2} \left(\frac{c_{11} + 4c_{12} - 2c_{44}}{2c_{11} + 3c_{12} + c_{44}} \right). \quad (44)$$

3 Validation and Analysis of the Twinning Criterion for FCC Materials

In this section we investigate the predictions of the twinning criterion derived in the previous section, including:

- (i) A comparison, for the crystallographic orientations in Table 3, to the atomistic results for aluminum of Hai and Tadmor (2003) – subsequently referred to as HT. The axes x_1 , x_2 and x_3 in the table are defined in Fig. 1. The table also gives the available slip systems for each orientation and the corre-

³ Lower values of $\gamma_{\text{sf}}/\gamma_{\text{us}}$ mean that emission of the trailing partial to complete a dislocation is more difficult, i.e. λ_{crit} becomes larger (see Fig. 4(a) and accompanying discussion). The dependence of T on $\gamma_{\text{us}}/\gamma_{\text{ut}}$ is obvious from (33).

Model	x_1	x_2	x_3	SP	θ	LP1 ϕ_{A1}	LP2 ϕ_{A2}	LP3 ϕ_{A3}
A	[111]	$[\bar{1}10]$	$[\bar{1}\bar{1}2]$	(111)	90°	B δ 30°	A δ 150°	C δ 270°
B	$[\bar{1}12]$	$[\bar{1}\bar{1}1]$	[110]	($\bar{1}\bar{1}1$)	0°	α D 60°	α B 180°	α C 300°
				($\bar{1}\bar{1}\bar{1}$)	70.53°	A β 0°	C β 120°	D β 240°
C	$[\bar{1}\bar{1}\bar{1}]$	[112]	$[\bar{1}\bar{1}0]$	(11 $\bar{1}$)	90°	γ D 0°	γ A 120°	γ B 240°
D	[121]	$[\bar{1}\bar{1}1]$	$[10\bar{1}]$	($\bar{1}\bar{1}1$)	0°	α D 0°	α B 120°	α C 240°
				(111)	109.5°	δ C 60°	δ A 180°	δ B 300°

Table 3

Crystallographic orientations, available slip planes (SP) and the three possible leading partial dislocations on each slip plane (LP1, LP2 and LP3) for the different crack configurations investigated. The Burgers vectors of the leading partials are given in Thompson vector notation (Hirth and Lothe, 1992).

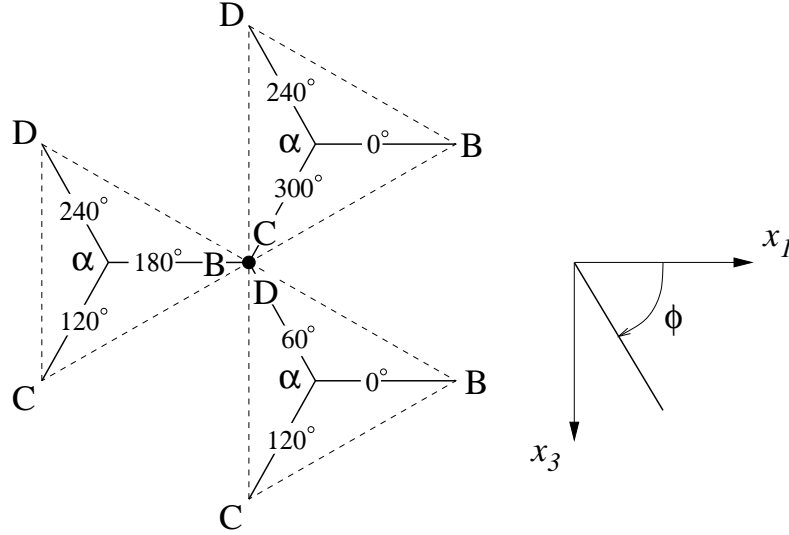


Fig. 5. Leading and trailing partial dislocation slip directions for the ($\bar{1}\bar{1}1$) slip plane of model B. Slip begins at the black circle in the center. For each slip direction, the angle ϕ is given along with the crystallographic orientation in Thompson notation.

sponding angles for the theoretical model. See HT for a detailed description of the crystallography of the slip systems.

- (ii) Construction of yield envelopes for model B in Table 3 for mixed mode II and III loading for aluminum and silver.

All of the results in this section involve the evaluation of the twinning criterion for fcc materials. It is well known that the active slip planes in fcc lattices are the $\{111\}$ planes with $\langle 112 \rangle$ partial dislocation directions. Each fcc slip plane has three possible leading partial directions ϕ_{A1} , ϕ_{A2} and ϕ_{A3} separated by 120° from each other. The three possible trailing partial directions are given by $\phi_{B1} = \phi_{A1} + 180^\circ$, $\phi_{B2} = \phi_{A2} + 180^\circ$ and $\phi_{B3} = \phi_{A3} + 180^\circ$. As an example, Fig. 5 shows the available leading and trailing partial directions for the ($\bar{1}\bar{1}1$)

Model/Loading	Critical Event	K_c [eV/Å ^{2.5}]
A/I	edge \perp (111) BA	0.142
B/I	twin (1 $\bar{1}\bar{1}$) Aβ	0.140
B/II	fault pair (1 $\bar{1}\bar{1}$) BD & BC	0.093
B/III	screw \perp (1 $\bar{1}\bar{1}$) CD	0.050
B/II-III (blunt)	mixed \perp (1 $\bar{1}\bar{1}$) BD	0.056
B/II-III (sharp)	twin (1 $\bar{1}\bar{1}$) αD	0.045
C/I	twin (11 $\bar{1}$) γD	0.210
D/II	twins (1 $\bar{1}\bar{1}$) αD and (111) Aδ	0.084

Table 4

Summary of the Quasicontinuum simulation results for aluminum. For each model/loading combination the event that occurred is listed along with the critical SIF at nucleation (K_c). The SIF values are given for the second partial dislocation emission which definitively determines whether a twin or a dislocation is nucleating. Reproduced from Hai and Tadmor (2003) with the exception of model D which is added here.

slip plane of model B. For a given loading mode, the twinning criterion needs to be tested for all available slip plane and slip direction combinations. The predicted deformation mode will be the one with lowest critical SIF.⁴

3.1 Comparison to atomistic simulations for aluminum

The configurations in Table 3 were simulated for fcc aluminum by HT using the quasicontinuum method (Tadmor et al., 1996; Shenoy et al., 1999) – a mixed continuum and atomistic approach. Aluminum is an interesting material to consider because despite being traditionally considered a material that does not exhibit DT (Venables, 1963), recent experimental evidence suggests that under certain conditions aluminum will deformation twin (Pond and Garcia-Garcia, 1981; Chen et al., 1999). Each of the crack models listed in Table 3 was simulated for a variety of loading modes. The resulting deformation mechanism (DT or dislocation emission) and the critical SIF were found. Table 4, reproduced from HT presents the simulation results. The simulations were performed using the EAM potential for aluminum due to Ercolessi and Adams (1993).

Model A corresponds to an orientation, previously studied by Hoagland et

⁴ A computer program, in Fortran 90 and MATLAB formats, for computing the twinning criterion for an fcc material may be downloaded from <http://tx.technion.ac.il/~tadmor>

al. (1990), where dislocation emission was observed under mode I loading. It was included in HT as a check on the simulation. Model B corresponds to an experimental configuration studied by Pond and Garcia-Garcia (1981) where DT was observed. The loading mode is not known in the experiment, therefore in the simulation the model is loaded in modes I, II and III as well as a mixed mode II and III with $\alpha = 60^\circ$. Under mode I loading a deformation twin is nucleated on the $(1\bar{1}\bar{1})$ plane. Under mode II loading an intrinsic-extrinsic fault pair is nucleated. This defect is formed by the reaction of two co-planar dissociated dislocations (**BC** and **BD**). The creation of the fault pair is thus considered to be a dislocation emission event. (See HT for a more detailed description of the fault pair structure.) Under mode III loading a screw dislocation is nucleated. Two crack tip morphologies were studied for the mixed mode case. The “sharp” crack tip is terminated by a (001) plane and the “blunt” crack tip is terminated by a $(1\bar{1}\bar{1})$ plane. The sharp and blunt terminology refers to the angle that the crack tip termination plane forms with the crack plane (54.7° for the sharp crack and 70.53° for the blunt crack). See HT for details. We see from Table 4 that the crack tip morphology strongly affects the resulting mode of deformation. For the blunt morphology a dislocation is nucleated, whereas for the sharp morphology a twin is nucleated with the same orientation as that observed in the experiment. Model C corresponds to an experimental configuration studied by Chen et al. (1999) where DT was observed under mode I loading. The simulation reproduces the experimental result. Model D is obtained by rotating model B about the x_2 -axis by 60° . This model did not appear in HT and is added here as an additional test for the criterion. The model was loaded in pure mode II using the same methodology described in HT. Two microtwins simultaneously nucleate, one on the $(1\bar{1}\bar{1})$ plane lying parallel to the crack plane and the other on the (111) plane lying at an angle of 109.471° to the crack plane.

To correctly interpret the atomistic simulation results it is necessary to understand the limitations of the methodology employed. The simulations were carried out under conditions of generalized plane strain. Atomistically this corresponds to a slab of material with thickness equal to the repeat distance in the out-of-plane direction and with periodic boundary conditions imposed in that direction. The implications of this constraint are:

- (i) Only dislocations with lines perpendicular to the simulation plane can nucleate. This constraint is consistent with the assumptions of the theoretical model.
- (ii) No variation along lines in the out-of-plane direction is possible. This means that nucleation of a dissociated screw dislocation composed of a leading and trailing partial is not possible in the simulation. Instead, a perfect undissociated screw dislocation will nucleate. This conclusion has important implications for the interpretation of the results, which are explained below.

Model/Loading	θ	ϕ_A	ϕ_B	T	sim	$K^\perp K^T$	K_{sim}	error
A/I	90°	30°	-30°	0.871*	⊥	0.219	0.142	54%
B/I	70.53°	0°	±60°	1.014	T	0.208	0.140	49%
B/II	0°	±60°	0°	0.871*	⊥	0.122	0.093	31%
B/III	0°	60°	120°	0.871*	⊥	0.070	0.050	40%
						(0.061)		(22%)
B/II-III (blunt)	0°	60°	0°	1.218	⊥	–	0.056	–
B/II-III (sharp)	0°	60°	0°	1.218	T	0.070	0.045	56%
C/I	90°	0°	±60°	1.014	T	0.216	0.210	3%
D/II	0°	0°	±60°	1.014	T	0.080	0.084	-5%

Table 5

Comparison of the predictions of the theoretical model and the numerical simulations of Hai and Tadmor (2003). See the text for an explanation of the quantities in the table. Results where DT is predicted or DT occurs in the simulation are bolded to highlight the agreement between theory and simulation. A * in the T column indicates that the trailing partial is predicted to nucleate spontaneously.

Table 5 summarizes the predictions of the twinning criterion for the investigated systems and compares them to the atomistic results. For each model and loading combination, the table includes the following information:

- (i) The angles of the active slip plane and slip directions (θ, ϕ_A, ϕ_B) as predicted by the criterion. Note that when DT is predicted ϕ_B refers to the trailing partial considered for the competing dislocation event, but no slip occurs along it.
- (ii) The predicted twinning tendency (recall $T > 1$ implies a twin should nucleate and $T < 1$ that a dislocation should) and the simulation result (“T” indicates a twin formed and “⊥” indicates a dislocation nucleated).
- (iii) The critical SIF for the nucleation event predicted by the criterion (dislocation emission K^\perp or twinning K^T), the simulation result K_{sim} and the error between them (SIF’s are given in units of eV/Å^{2.5}).

Qualitative assessment of the twinning criterion

Qualitatively, the criterion predicts the correct result in each case with the exception of model B/II-III where the simulated result depends on the crack tip morphology. In all other cases, whenever the theory predicted $T > 1$, DT was observed in the simulation and whenever $T < 1$, dislocation emission was observed. In addition, in all cases, the active slip system predicted by the criterion was the one observed in the simulation. Several of the results require additional explanation.

θ	ϕ_A	ϕ_B	T	$K^\perp K^T$
0.00°	60.00°	120.00°	0.995	0.0695
0.00°	60.00°	0.00°	1.218	0.0699
70.53°	120.00°	60.00°	0.871	0.0994
70.53°	120.00°	180.00°	>10	0.1141

Table 6

Evaluation of the twinning criterion for model B loaded in mixed mode II and III with $\alpha = 60^\circ$ for all possible slip systems. Only systems where defect nucleation is predicted are listed. The critical SIF is in units of $\text{eV}/\text{\AA}^{2.5}$. The results are sorted by the critical SIF for the event.

For model B/III the criterion predicts the nucleation of a dissociated screw dislocation $\alpha\mathbf{D}+\mathbf{C}\alpha=\mathbf{CD}$ at $K_{\text{III}} = 0.070 \text{ eV}/\text{\AA}^{2.5}$. As explained above this mode of deformation is not possible in the simulation. It is more appropriate to compare the simulation result for the SIF required to nucleate a perfect screw dislocation \mathbf{CD} along the $[110]$ direction. The critical load is obtained from (5) by substituting in $\phi_A = 90^\circ$ and γ_{us}^{110} , the unstable stacking energy for slip along a $\langle 110 \rangle$ direction, giving $K_{\text{III}} = \sqrt{2\mu\gamma_{\text{us}}^{110}}$. For the Ercolessi and Adams (1993) potential for aluminum, $\gamma_{\text{us}}^{110}=27.05 \text{ meV}/\text{\AA}^2$ (a significantly higher barrier than γ_{us}) and the critical emission SIF is $K_{\text{III}}=0.061 \text{ eV}/\text{\AA}^{2.5}$. This value is much closer to that observed in the simulation.

For model B/II-III the criterion predicts the emission of a dissociated screw dislocation, with $T=0.995$ and $K=0.0695 \text{ eV}/\text{\AA}^{2.5}$. In the simulation this result is not observed for either crack morphology. For the blunt crack a mixed dissociated dislocation $\alpha\mathbf{D}+\mathbf{B}\alpha=\mathbf{BD}$ at a 30° angle to the x_1 axis is nucleated. For the sharp crack a twin $\alpha\mathbf{D}$ at a 60° angle to the x_1 axis is nucleated. The discrepancy is again tied to the inability of the simulation to nucleate a dissociated screw dislocation. Taking this constraint into account, the SIF for nucleating the undissociated screw dislocation is given by $K = \sqrt{8\mu\gamma_{\text{us}}^{110}/3}$. This relation is obtained from (25) by substituting in $\alpha = 60^\circ$ and $\phi_A = 90^\circ$. For Ercolessi and Adams (1993) aluminum the critical SIF is $K=0.122 \text{ eV}/\text{\AA}^{2.5}$, which is larger than other competing mechanisms (Table 6). With screw dislocation nucleation thus ruled out, the next likely deformation mechanism predicted by the criterion is DT at $K=0.0699 \text{ eV}/\text{\AA}^{2.5}$. This mode of deformation agrees with the simulation result for the sharp crack morphology but not for the blunt morphology. The reason for this is discussed later when ledge effects are considered. The fact that the theoretical model predicts screw dislocation nucleation and not DT for model B/II-III is surprising since the loading direction exactly coincides with the leading partial direction. It seems reasonable to expect that it would be easier to nucleate another partial along this direction to form a microtwin instead of a trailing partial at a 60° angle. The reason that this does not occur is tied to Poisson's ratio. As can be seen in Fig. 4(b)

ν can have a strong effect on the load required to nucleate the trailing partial. In this case Poisson's ratio is just large enough to make the nucleation of the trailing partial more favorable.

For model D the criterion predicts DT on the $\theta = 0$ plane, which is also observed in the simulation. However, in the simulation an additional microtwin nucleates on the $\theta = 109.5^\circ$ plane. The criterion predicts DT for this plane as well but at a higher SIF of $K_{II} = 0.139 \text{ eV}/\text{\AA}^{2.5}$.

Quantitative assessment and sources of error

While qualitatively the criterion is able to predict the correct mode of deformation in every case, quantitatively it is less successful, with errors ranging from 5% to 56%. The errors for cases where DT occurs are of the same order as those where dislocation emission occurs. The sources of error in Rice's model for dislocation emission have been extensively studied and are briefly reviewed below. It has been shown that these errors can be systematically reduced by various extensions to the basic model. It is presumed that the same is true for the twinning model, but this requires further work to verify.

In general, the errors for cases where nucleation is on an inclined plane are higher than those where nucleation is on the plane coincident with the crack plane. Two exceptions to this behavior are models B/II-III, where the error is large despite the fact that nucleation occurs on the $\theta = 0$ plane, and model C/I where the error is very low. The low error for model C/I is most likely related to the fact that, in the simulation, mesh adaption was not activated for this particular model and as a result boundary effects probably retarded the nucleation event. See HT for details. It is not clear why the emission load in model B/II-III is overpredicted, but we note that this is the only model where a twin is nucleated at an angle to the crack direction ($\phi_A = 60^\circ$). This fact suggests that the error may be related to anisotropic effects neglected in the current formulation, as explained below.

The larger errors observed for nucleation on inclined planes is most likely related to the effective SIF approach. The effect of this approximation on the nucleation loads was studied by Rice et al. (1992). An exact solution for the case of $\theta \neq 0$ was derived by enforcing equilibrium on the inclined plane and solving the resulting integral equation. The authors find that the effective SIF approach overestimates the critical nucleation loads with the error reaching about 25% when $\theta = 90^\circ$. For the current analysis the average error for models where nucleation occurred on an inclined plane (discounting model C/I) were about 15% higher than the average error for cases where nucleation occurred on a coincident plane. This error difference is well within the range observed for this effect.

The effect of anisotropy was studied by Sun and Beltz (1994). The authors find that anisotropic effects may increase or decrease the nucleation load based on the material, crystallographic orientation and loading mode. For fcc metals, the nucleation loads can change by as much as 25%. The effect scales with the anisotropy ratio $A = 2c_{44}/(c_{11} - c_{22})$ ($A = 1$ for an isotropic material). This value is relatively low for aluminum ($A=1.32$ for Ercolessi and Adams (1993) aluminum) so anisotropic effects are not expected to dominate in this case. However, this is the most likely source for the large error in model B/II-III where nucleation occurred on the plane coincident with the crack plane.

The effect of the coupling between slip and opening displacement along the slip direction, referred to as shear-tension coupling, was studied by Sun et al. (1993). The authors find that neglecting this effect can result in significant overprediction of the critical nucleation loads. For aluminum the errors can be as large as 20% (Rice et al., 1992). Use of the relaxed γ_{us} value (as is done here) improves accuracy somewhat but errors can still be large. The authors show that accuracy is improved by using a modified unstable stacking energy $\gamma_{\text{us}}^{(u^*)}$ which is the unstable stacking energy for planes which are constrained to slip at a fixed opening displacement corresponding to the relaxed opening at the unstable configuration. It remains to be seen whether a similar correction may be used for the unstable twinning energy.

Finally, Juan et al. (1996) studied the effect of ledge energy on the nucleation load. Ledge effects were included by carrying out the GSF surface calculation on an ingenious supercell which automatically included the ledge structure. From the calculations the authors extract the ledge surface energy $\tilde{\gamma}_s$ which due to corner effects is lower than the surface energy γ_s for the ledge orientation. Rice's model was then extended to include the effect and it was found that the change to the energy release rate due to ledge effects scales linearly with $\tilde{\gamma}_s$. Depending on the ratio $\tilde{\gamma}_s/\gamma_s$ the corresponding nucleation load can increase by as much as 20%.

The ledge energy effect deserves special mention for the case of DT. Unlike dislocation emission where the only additional penalty to nucleating the dislocation is the energy of the ledge that is formed at the crack tip, for the case of DT an additional *edge* effect is present due to the formation of an incoherent twin boundary at the tip of the twin. This boundary is a high-energy defect and its contribution to the energy balance of the twin formation may be significant. The possibility of the reduction of the tip energy by dislocation reactions leading to the formation of residual and emissary dislocations must also be considered in this case (Hirth and Lothe, 1992; Pond and Garcia-Garcia, 1981; Christian and Mahajan, 1995).

The importance of including edge and ledge effects in the model is demonstrated by model II/III where the resulting mode of deformation was con-

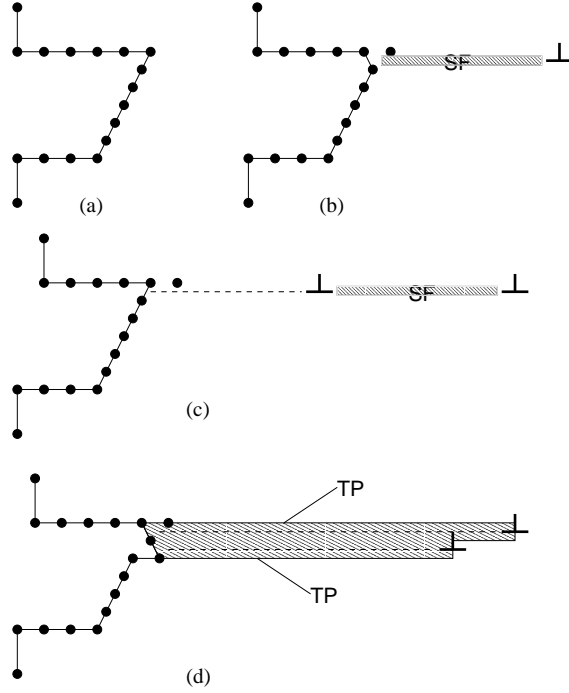


Fig. 6. Schematic representation of dissociated dislocation nucleation versus deformation twinning for the blunt crack tip morphology. The figure is drawn for an fcc material with a $\{111\}$ crack plane and a $\langle 110 \rangle$ crack direction with the crack terminated by a $\{111\}$ plane. For an explanation of the frames and notation, see Fig. 2.

trolled by the crack tip morphology. This effect is explained in Fig. 6 which schematically shows the competition between dislocation emission and DT for the blunt crack morphology. This figure should be compared with Fig. 2 which shows the same competition for the sharp crack morphology. The ledge formed in the blunt crack is energetically more expensive than that of the sharp crack. This suggests that in model B/II-III ledge effects are the controlling factor in determining the resulting mode of deformation. The theoretical model, which neglects ledge effects in its current form, predicts DT in accordance with the sharp crack results where the ledge effect is smaller. To differentiate between the sharp and blunt morphologies, the theoretical model will have to be extended to include ledge effects.

3.2 Mixed mode II and III yield envelopes

In the previous section the predictions of the twinning criterion for aluminum for a number of different configurations was investigated. The results were found to strongly depend on the crystallographic orientation and loading direction. For model B, for example, the criterion predicts the emission of a mixed dislocation for mode II ($\alpha = 0^\circ$), a screw dislocation for mode III

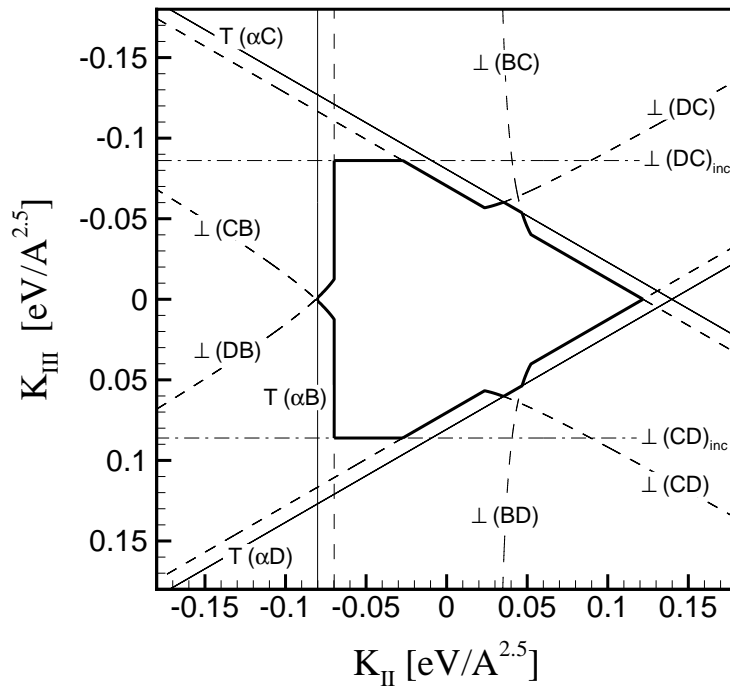
($\alpha = 90^\circ$) and a twin for a mixed mode II and III loading with $\alpha = 60^\circ$. Given this complexity it is of interest to plot the yield envelope for shear loading in the x_1 - x_3 plane to see the defect predicted to nucleate at an arbitrary angle α .

The yield envelopes for aluminum and silver in orientation B are given in Figs. 7(a) and 7(b), respectively. The K_{III} axis has been reversed in order to agree with the direction of the x_3 axis which is positive downwards when viewed down along the x_2 axis. Each line in the figures corresponds to the critical K_{II} - K_{III} combination necessary to nucleate a specific defect. The type of defect formed (\perp or T) and its Burgers vector are indicated somewhere along the line (see Fig. 5 for clarification of the slip directions). The innermost contour of the defect nucleation lines is indicated by a thick line and constitutes the yield envelope of the material. For K_{II} - K_{III} combinations lying inside this envelope no defects will form and the deformation will be purely elastic. Only defect lines that contribute to the yield envelope are included in the plots. Solid lines correspond to microtwin nucleation and broken lines to nucleation of the trailing partial which completes a dissociated dislocation. The lines corresponding to the emission of the leading partials have been omitted from the figure to reduce clutter. These lines lie very close to the yield envelope – either directly on top of it or slightly to the inside. Most of the lines forming the yield envelope correspond to defects nucleated on the $(1\bar{1}1)$ plane coincident with the crack plane. The exceptions are the horizontal dash-dot lines which are associated with the nucleation of **CD** and **DC** screw dislocations on the inclined $(1\bar{1}\bar{1})$ plane.

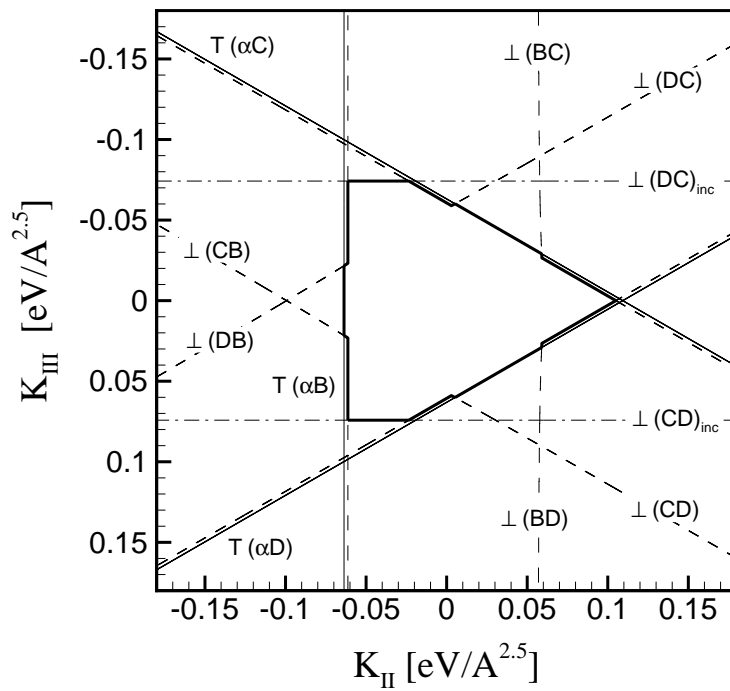
The yield envelopes for both materials are roughly triangular and pointing to the right. The shape of the envelopes is directly tied to the available slip directions in the $(1\bar{1}1)$ plane (Fig. 5) which share the same symmetries. Most of the envelope corresponds to yielding by nucleation of dislocations of various types. DT is predicted at the three raised flat regions located at about $\pm 60^\circ$ and at 180° relative to the horizontal axis. Comparing the yield envelopes of aluminum and silver it is clear that the region where DT occurs relative to dislocation emission is far smaller in aluminum than in silver. This is consistent with what is known experimentally regarding these materials, namely that aluminum rarely twins while silver twins far more readily.

4 Conclusions

A criterion for the onset of deformation twinning at a crack tip has been derived based on the Peierls concept. The criterion is obtained by considering the competing mechanisms at the crack tip after a leading partial dislocation has been emitted. Emission of a trailing partial will result in the nucleation of



(a)



(b)

Fig. 7. Yield envelope for (a) aluminum and (b) silver. See text for explanation.

a dissociated perfect dislocation whereas emission of a second leading partial on an adjacent plane will result in the nucleation of a two-layer microtwin which is taken to be a precursor to DT. The critical SIF's for the nucleation of the leading and trailing partials were obtained by Rice (1992). The critical SIF for nucleation of the twinning partial is obtained here using a similar approach. It is found that the nucleation of the twinning partial is controlled by the *unstable twinning energy* γ_{ut} . This new material parameter is analogous to Rice's unstable stacking energy, γ_{us} , which controls the leading partial emission. γ_{ut} is the maximum energy encountered, when in a crystal containing an intrinsic stacking fault, the part of the crystal one layer above the stacking fault is rigidly displaced along the twinning partial direction. Numerical values for γ_{ut} were computed for three fcc materials (aluminum, copper and silver) using EAM potentials.

The competition between dislocation emission and DT at the crack tip is quantified by the *twinning tendency* T defined as the ratio of the critical SIF for dislocation nucleation K^\perp and the critical SIF for the formation of a microtwin K^T , $T \equiv K^\perp/K^T$. DT is predicted when $T > 1$ and dislocation emission when $T < 1$. When the external loading is proportional to a single load parameter (i.e. $(K_{\text{I}}, K_{\text{II}}, K_{\text{III}}) \propto K$), the twinning tendency is found to have a particularly simple form, $T = \lambda_{\text{crit}} \sqrt{\gamma_{\text{us}}/\gamma_{\text{ut}}}$. In this expression, λ_{crit} represents the additional load necessary to nucleate the trailing partial relative to the leading partial ($\lambda_{\text{crit}} = K^\perp/K^1$ where K^1 is the critical SIF for nucleation of the leading partial). λ_{crit} is a function of the angles characterizing the available slip systems (θ, ϕ_A, ϕ_B), the loading direction α , Poisson's ratio ν and the intrinsic stacking fault to unstable stacking energy ratio $\gamma_{\text{sf}}/\gamma_{\text{us}}$. It does not depend on the shear modulus μ . For fcc metals, λ_{crit} increases with decreasing values of $\gamma_{\text{sf}}/\gamma_{\text{us}}$. This means that materials with low $\gamma_{\text{sf}}/\gamma_{\text{us}}$ ratios are more likely to twin. The second term in the twinning tendency expression is the unstable stacking to unstable twinning energy ratio $\gamma_{\text{us}}/\gamma_{\text{ut}}$. This ratio which is less than one characterizes the difficulty of DT relative to dislocation emission. The smaller this ratio is the more difficult it is for a material to twin. The dependence of λ_{crit} on the stacking fault energy ratio is consistent with experimental findings that show that the twin nucleation stress decreases with decreasing values of the intrinsic stacking fault energy (Venables, 1963). However, these experimental findings have led to the general belief that the tendency of a material to twin is primarily controlled by the intrinsic stacking fault energy, which the current model shows is only partly correct.

The predictions of the criterion are compared with the atomistic simulations for aluminum of (Hai and Tadmor, 2003) for a number of different crack configurations and loading modes. The criterion is found to be qualitatively exact for all cases, predicting the correct deformation mode (DT vs. dislocation emission) and the correct activated slip system. Quantitatively the accuracy of the predicted nucleation loads varies from 5% to 56%. Errors were larger

when nucleation occurred on slip planes inclined relative to the crack plane. The errors for cases where DT occurs are of the same order as those where dislocation emission occurs. The sources of errors of Rice's model for dislocation emission have been extensively studied and include the effective SIF approximation for nucleation on inclined planes (Rice et al., 1992), shear-tension coupling effects (Sun et al., 1993), anisotropic effects (Sun and Beltz, 1994) and ledge energy effects (Juan et al., 1996). For DT an additional *edge* effect needs to be considered due to the creation of an incoherent twin boundary at the tip of the twin. By including these effects, the errors can be systematically reduced in the dislocation model and it is presumed that the same is true for the twinning model, but this requires further study.

In addition to limitations of the basic model discussed above, several important aspects of DT have been neglected in the present formulation. First, temperature effects are absent from the model. Thermal activation is not thought to play an important role in DT (Christian and Mahajan, 1995) and thus the prediction of the model for the critical SIF for DT may be reasonable. However, dislocation emission is sensitive to thermal effects. It is well-known that DT becomes more favorable over slip at lower temperatures (Christian and Mahajan, 1995). This trend cannot be obtained from the present formulation. Second, strain rate effects, which have been shown to be very important for DT (Christian and Mahajan, 1995), are absent from the model. Materials twin far more readily at high strain rates than at low strain rates. This is often quoted as a reason why deformation twins nucleate at the tips of moving cracks where large stresses and strain rates are present (Reid, 1981).

Future work should focus on (1) reduction of errors by considering the sources of error discussed above; (2) more exact calculation of γ_{ut} using first-principles quantum mechanical calculations; (3) validation of the assumption that a microtwin can be considered a twin precursor by explicitly considering the nucleation of twinning partials on layers adjacent to the microtwin; and (4) application of the theory to bcc and hcp materials where DT is a prevalent mode of deformation.

Acknowledgement We are grateful to W. Kaplan for carefully reading the original thesis this manuscript is based on and for his helpful comments. We would also like to thank J. Zimmerman for his assistance in obtaining some of the EAM potentials used in our analysis, and R. Miller for reviewing parts of the derivation.

References

Bilby, B. A., Bullough, R., 1954. The formation of twins by a moving crack. *Philosophical Magazine* 45, 631-646.

- Bošanský, J., Šmida, T., 2002. Deformation twins – probable inherent nuclei of cleavage fracture in ferritic steels. *Materials Science and Engineering A323*, 198-205.
- Chen, Q., Huang, Y., Qiao, L., Chu, W., 1999. Failure modes after exhaustion of dislocation glide ability in thin crystals. *Science in China (Series E)* 42, 1-9.
- Christian, J. W., Mahajan, S., 1995. Deformation twinning. *Progress in Materials Science* 39, 1-157.
- Daw, M. S., Baskes, M. I., 1983. Semiempirical, quantum-mechanical calculations of hydrogen embrittlement in metals. *Physical Review Letters* 50, 1285-1288.
- Deruyttere, A., Greenough, G. B., 1954. The markings in the cleavage surfaces of zinc single crystals. *Philosophical Magazine* 45, 624-630.
- Dève, H. E., Evans, A. G., 1991. Twin toughening in titanium aluminide. *Acta Metallurgica and Materialia* 39, 1171-1176.
- Ercolessi, F., Adams, J., 1993. Interatomic potentials from 1st-principles calculations – the force-matching method. *Europhysics Letters* 26, 583-588.
- Hai, S., Tadmor, E. B., 2003. Deformation twinning at aluminum crack tips. *Acta Materialia* 51, 117-131.
- Hammer, B., Jacobsen, K. W., Millman, V., Payne, M. C., 1992. Stacking fault energies in aluminum. *Journal of Physics: Condensed Matter* 4, 10453-10460.
- Hirth, J. P., Lothe, J., 1992. *Theory of Dislocations*, Second Edition. Krieger Publishing Company, Malabar.
- Hoagland, R. G., Foiles, S. M., Baskes, M. I., Daw, M. S., 1990. An atomic model of crack tip deformation in aluminum using an embedded atom potential. *Journal of Materials Research* 5, 313-324.
- Jagannadham, K., Armstrong, R. W., Hirth, J. P., 1993. Deformation twinning in high-hydrogen-solubility refractory alloy crystals. *Philosophical Magazine A* 68, 419-451.
- Juan, Y.-M., Sun, Y., Kaxiras, E., 1996. Ledge effects on dislocation emission from a crack tip: a first-principles study for silicon. *Philosophical Magazine Letters* 73, 233-240.
- Lebensohn, R. A., Tomé, C. N., 1993a. A study of the stress state associated with twin nucleation and propagation in anisotropic materials. *Philosophical Magazine A* 67, 187-206.
- Lu, G., Kioussis, N., Bulatov, V. V., Kaxiras, E., 2000. Generalized-stacking-fault energy surface and dislocation properties of aluminum. *Physical Review B* 62, 3009-3108.
- Miller, R., Tadmor, E. B., Phillips, R., Ortiz, M., 1998. Quasicontinuum simulation of fracture at the atomic scale. *Modelling and Simulation in Materials Science and Engineering* 6, 607-638.
- Peierls, R. E., 1940. The size of a dislocation. *Proceedings of the Physical Society of London* 52, 34-37.
- Paxton, A. T., Gumbsch, P., Methfessel, M., 1991. A quantum mechanical

- calculation of the theoretical strength of metals. *Philosophical Magazine Letters* 63, 267-274.
- Pond, R. C., Garcia-Garcia, L. M. F., 1981. Deformation twinning in aluminum. *Institute of Physics Conference Series*, No. 61, 495-498.
- Reid, C. N., 1981. The association of twinning and fracture in bcc metals. *Metallurgical Transactions A* 12A, 371-377.
- Rice, J. R., 1968. A path independent integral and the approximate analysis of strain concentration by notches and cracks. *Journal of Applied Mechanics* 35, 379-386.
- Rice, J. R., 1992. Dislocation nucleation from a crack tip: an analysis based on the Peierls concept. *Journal of the Mechanics and Physics of Solids* 40 (2), 239-271.
- Rice, J. R., Beltz, G. E., Sun, Y., 1992. Peierls framework for dislocation nucleation from a crack tip. In: Argon, A. S. (Ed.), *Topics in Fracture and Fatigue*. Springer-Verlag, p. 1.
- Shenoy, V. B., Miller R., Tadmor, E. B., Rodney, D., Phillips, R., Ortiz, M.R., 1999. An adaptive finite element approach to atomic-scale mechanics – the quasicontinuum method. *Journal of the Mechanics and Physics of Solids* 47, 611-642.
- Sun, Y. M., Beltz, G. E., Rice, J. R., 1993. Estimates from atomic models of tension-shear coupling in dislocation nucleation from a crack tip. *Materials Science and Engineering A* 170, 67-85.
- Sun, Y. M., Beltz, G. E., 1994. Dislocation nucleation from a crack tip – a formulation based on anisotropic elasticity. *Journal of the Mechanics and Physics of Solids* 42, 1905-1932.
- Suresh, S., 1991. *Fatigue of Materials*. Cambridge University Press, Cambridge.
- Tadmor, E. B., Ortiz, M., Phillips, R., 1996. Quasicontinuum analysis of defects in solids. *Philosophical Magazine A* 73, 1529-1563.
- Venables, J. A., 1963. Deformation twinning in fcc metals. In: Reed-Hill, R. E.(Ed.), *Deformation Twinning*. Proceedings of the Metallurgical Society Conference (vol. 25). Gordon and Breach Science Publishers, p. 77.
- Vitek, V., 1968. Intrinsic stacking faults in body-centered cubic crystals. *Philosophical Magazine* 18, 773-786.
- Voter, A. F., 1994. The Embedded Atom Method. In: Westbrook, J. H., Fleischer, R. L. (Eds.), *Intermetallic Compounds: Principles* (vol. 1). Wiley, p. 77.
- Yoo, M. H., 1979. A dislocation model for twinning and fracture and its application to hcp metals. In: Haasen, P., Gerold, V., Kostorz, G. (Eds.), *Proceedings of the Fifth International Conference on the Strength of Metals and Alloys* (Vol. 2). Pergamon, p. 825.
- Yoo, M. H., 1981. Slip, twinning and fracture in hexagonal close-packed metals. *Metallurgical Transactions A* 12A, 409-417.
- Yoo, M. H., 1998. Twinning and mechanical behavior of titanium aluminides and other intermetallics. *Intermetallics* 6, 597-602.